FISH and FISHERIES

**ORIGINAL ARTICLE** OPEN ACCESS

# Bottom-Up Interactions in State-Space Age-Structured Models Using Mass-Balance Dynamics

James T. Thorson[1] | Kerim Y. Aydin[1] | Matthew L. H. Cheng[2] | Beatriz S. Dias[3] | David G. Kimmel[4] |
Kasper Kristensen[5]

[1]Resource Ecology and Fisheries Management, Alaska Fisheries Science Center, National Marine Fisheries Service, NOAA, Seattle, Washington, United States | [2]Department of Fisheries at Lena Point, College of Fisheries and Ocean Sciences, University of Alaska Fairbanks, Juneau, Alaska, USA | [3]Cooperative Institute for Climate, Ocean, and Ecosystem Studies, University of Washington, Seattle, Washington, USA | [4]Recruitment Process Program, Alaska Fisheries Science Center, NOAA, NMFS, Seattle, Washington, USA | [5]Technical University of Denmark, Lyngby, Denmark

**Correspondence:** James T. Thorson (james.thorson@noaa.gov)

**ABSTRACT**

Age-structured models are used worldwide to regulate fisheries. These models typically ignore top-down interactions (predation affecting natural mortality) and bottom-up interactions (consumption affecting individual growth, reproduction, or survival), whereas multispecies catch-at-age models often incorporate top-down but not bottom-up interactions. While Ecopath-with-Ecosim (EwE) incorporates both top-down and bottom-up interactions along with age-structured dynamics, it is not typically fitted to age-composition data. We extend Ecostate (a state-space version of EwE) to incorporate age-structured dynamics while fitting to age-structured data and use this to illustrate how to add bottom-up interactions to age-structured models. Specifically, we add age-structured dynamics and likelihood components for age-composition and weight-at-age data while estimating residual variation in larval survival (recruitment deviations) and consumption (weight-at-age deviations). As a demonstration, we fit the model to biomass and age-composition data for two commercial species (Alaska pollock and sablefish) in the Gulf of Alaska, including population dynamics for their major prey, while not fitting weight-at-age data so that it can be used for out-of-sample evaluation of model performance. The model can be viewed as a multispecies age-structured model (e.g., estimating adult mortality rates, survey catchability and selectivity, and recruitment variation) and as a mass-balance ecosystem model (e.g., estimating trophic position and weight-at-age based on forage consumption). The predicted weight-at-age is weakly correlated with independent measurements for pollock and sablefish but was improved when we incorporated forage biomass indices. We recommend that age-structured models routinely explore the link between prey consumption and resulting size-at-age, whether using coupled predator–prey dynamics or simplifications that treat prey abundance as fixed data.

## 1 | Introduction

Animal populations allocate energy for growth, reproduction, and activity that is limited by their access to prey forage ("bottom-up control"), and survival rates may decline as population sizes increase due to predator responses ("top-down control"). Decades of research have sought to quantify the relative importance of these two in regulating ecosystem dynamics (see Leroux and Loreau

2015 for a review). However, interest in "bottom-up interactions" in marine ecosystems is growing for several reasons:

1. *Climate change*: Primary production is changing due to global temperature and nutrient supply (Boyce and Worm 2015), and regional changes in primary production may impact ecosystem-level sustainable harvest (Atkinson et al. 2024; Chassot et al. 2010);

---

2. *Managing harvest for forage species*: Alternatively, direct harvest of forage species such as Atlantic menhaden (Chagaris et al. 2020) and Antarctic krill (Trathan et al. 2022) has led managers to regulate the harvest of forage species based on their impact on other fished or protected species;

3. *Change in size*: A change in forage abundance and consumption can lead to decreased size-at-age for a commercially important fish, as well documented, e.g., for Baltic cod (Neuenfeldt et al. 2020).

Given these varied motivations, there is a need for analytical methods that can inform ocean managers about likely trade-offs resulting from "bottom-up" interactions.

Bottom-up drivers are typically analysed using mass-balance or "end-to-end" ecosystem models that are generally not fitted directly to time-series data. For example, the mass-balance model Ecopath is typically balanced by estimating an unknown "ecotrophic efficiency" (the fraction of mortality rates attributed to modelled predators) given specified values for production and consumption per biomass as well as biomass and diet proportions for a list of interacting species (Polovina 1984). Ecopath can then be projected over time using Ecosim (Walters et al. 1997), and Ecosim can incorporate age-structured dynamics (Walters et al. 2000) which then have important consequences for species interactions (Walters and Kitchell 2001). Predator functional-response parameters are sometimes estimated via fit to time-series data without otherwise fitting parameters in the original Ecopath mass-balance (Bentley et al. 2024; Scott et al. 2016). However, Ecopath parameters are not typically estimated via fit to time-series data and, as a result, achieving mass-balance within Ecopath can be a time-consuming part of model construction.

When fitting model dynamics to time-series data, analysts can instead apply integrated stock assessment models (Punt et al. 2020). For example, age-structured stock-assessment models (ASSAM) are typically fitted to survey and fishery data and then used to predict the likely impact of alternative fishery regulation on future biomass and harvest (Methot 2009). Alternatively, multispecies statistical catch-at-age models (MSSCA) extend ASSAM by estimating biomass for multiple species and then incorporate "top-down" drivers by predicting variation in natural mortality for a prey species based on the consumption by their predators (Begley and Howell 2004; Jurado-Molina et al. 2005). Despite their widespread use, ASSAM and MSSCA typically do not estimate "bottom-up" drivers, i.e., how prey biomass and resulting consumption subsequently affect the productivity (i.e., growth, reproduction, or survival) of their predators. Exceptions exist, however, including bespoke models estimating the impact of consumption on e.g., individual growth via bioenergetics (Fitzpatrick et al. 2022) or biomass growth rates (Tulloch et al. 2019).

Both ecosystem and stock assessment models are used worldwide to manage ocean ecosystems. Fisheries managers generally establish and implement harvest control rules using information from stock assessment models (Methot 2009); research confirms that this is an important contributor to effective fisheries governance (Melnychuk et al. 2021). Fisheries managers

in the eastern Bering Sea also established a system-wide limit on total harvest derived from ecosystem modelling, and it has been effective for decades in mitigating stakeholder conflicts. Similarly, Atlantic menhaden is currently managed using catch advice from a mass-balance model (Chagaris et al. 2020), and the ICES WKIrish workshop endorsed EwE for use in management in the Irish Sea (Bentley et al. 2021). However, Karp et al. (2023) list eight challenges in the wider use of ecosystem models for fisheries management, including proper review and reproducibility for ecosystem models. By fitting directly to data, stock assessment models can be routinely updated to support annual management, such as a harvest control rule, and can be independently reproduced or reviewed by any interested party. Fitting directly to time-series data could presumably provide a similar role for ecosystem models.

More recently, there has been increased research regarding state-space versions of MSSCA and ASSAM, which incorporate both variation in measurements ("measurement error") and variation in demographic rates over time ("process errors"). For example, state-space ASSAM has been developed to estimate changes in weight-at-age (Correa et al. 2023), and state-space MSSCA can estimate process errors in recruitment for individual species (Adams et al. 2022). Similarly, Ecostate was developed as a state-space extension to mass-balance dynamics, e.g., EwE, and it represents both bottom-up and top-down drivers for biomass dynamics across producers, consumers, and detritus (Thorson et al. 2024). It is fitted directly to time-series data, can include Bayesian priors on difficult-to-estimate parameters, and is available using package *ecostate* on the Comprehensive R Archive Network (CRAN) with vignettes and documentation, facilitating simulation experiments to test its likely performance. However, Ecostate was restricted to modelling biomass dynamics without age-structure, and therefore did not fit age-composition data, estimate recruitment variation, track cohort strength, estimate fishery selectivity, or incorporate other features that are common in ASSAM.

In this paper, we discuss how to incorporate bottom-up interactions into statistical age-structured models by linking individual growth of predators to population-level consumption of their prey, and demonstrate the approach by extending Ecostate to include age-structured dynamics. We first outline how simple metabolic assumptions can link individual size-at-age to population-level consumption. We then summarise Ecostate and outline how it predicts weight-at-age from theory (biomass dynamics) and/or observations (biomass indices) for forage species. We then demonstrate the model by fitting to two age-structured populations (sablefish *Anoplopoma fimbria* and walleye pollock *Gadus chalcogrammus*) as well as their major forage pathways (pelagic production and benthic detritus via copepods and euphausiids) in the Gulf of Alaska. We evaluate model performance by (1) withholding real-world measurements of weight-at-age and comparing these with model predictions of weight-at-age; (2) withholding and then forecasting later biomass index and age-composition data in a retrospective skill-testing experiment; and (3) evaluating how model performance changes when withholding survey indices for zooplankton forage. Our analysis demonstrates that state-space mass-balance models serve as a useful middle ground between stock and ecosystem modelling, and can attribute predator growth to their consumption of prey.

## 2 | Methods

We seek to add bottom-up interactions to age-structured models by linking individual growth (and resulting size-at-age) to population consumption. We seek a method that can be repurposed in a large number of other population-dynamics models; therefore, we use (1) age-structured dynamics, given its wide usage in age-structured stock assessment models, and (2) measurements of consumption in biomass (e.g., mass-balance models) because biomass is already estimated in most age-structured stock assessments. In the following, we adapt an approach derived from Ecopath with Ecosim (Lucey et al. 2020; Walters et al. 1997) and in particular Ecosim's multistanza extension (Walters et al. 2000) that can be repurposed in state-space mass balance and age-structured assessment models.

The proposed method requires:

1. Weight-at-age represented using the generalised von Bertalanffy function in a selected ("reference") time;

2. Consumption and metabolic demand that result in weight-at-age in that reference time;

3. Consumption and metabolic demand during a given time interval are used to calculate growth increments in that interval relative to the reference time.

In the following, we define reference weight-at-age, consumption, and metabolic demand as values that occur in a model equilibrium (see Table S1 for a list of notation, or the "ecostate model description" vignette[1]). However, future studies could apply the method to models without a defined equilibrium, and instead define growth relative to some initial consumption and weight-at-age. We proceed by first reviewing the theory from which this method is derived.

### 2.1 | Individual Growth and Population Consumption

Fish grow based on the balance between energetic supply (anabolism) and expenditure (catabolism), and Bertalanffy (1969 Eq. 7.8) formalised this by theorising that an animal with body size $\omega$ (in units mass) has growth rate $\frac{d}{dt}\omega$ that follows a differential equation[2]:

$$\frac{d}{dt}\omega = \underbrace{H\omega^d}_{\text{Anabolism}} - \underbrace{K\omega}_{\text{Catabolism}} \tag{1}$$

where $d$ is the allometric increase in consumption with body size, $H$ is the consumption per effective size, and $K$ is the linear increase in catabolism with body mass (Essington et al. 2001). Integrating this expression over time, where individuals start at zero mass (i.e., $\omega(0) = 0$) then results in the generalised von Bertalanffy growth function:

$$\omega(a) = \omega_\infty \left(1 - e^{K(1-d)a}\right)^{\frac{1}{1-d}} \tag{2}$$

where asymptotic weight $\omega_\infty = \left(\frac{H}{K}\right)^{\frac{1}{1-d}}$. When assuming that body mass scales isometrically (i.e., $\omega = aL^b$ where $b = 3$) and that consumption increases with length-squared (i.e., $d = 2/3$), this expression reduces to the widely used von Bertalanffy model for length-at-age $L(a) = L_\infty\left(1 - e^{-ka}\right)$ where $k = 3K$.

Although the von Bertalanffy length-at-age function is widely used in age-structured stock-assessment models, there are relatively few models that incorporate bottom-up interactions by linking individual growth rate $\frac{d}{dt}\omega$ (or growth increments using a linear approximation to $\frac{d}{dt}\omega$) to consumption. To make this link, let us first assume that a population has an equilibrium weight-at-age $\overline{\omega}_a$ that arises from the generalised von Bertalanffy growth function (Equation 2). We also calculate the equilibrium age distribution $\overline{v}_a$, and define biomass $\beta = \sum_{a=0}^{a_{\max}} v_a \omega_a$ such that the equilibrium biomass $\overline{\beta} = \sum_{a=0}^{a_{\max}} \overline{v}_a \overline{\omega}_a$.

We start by applying an Euler (piecewise linear) approximation to the von Betalanffy differential equation (Equation 1) for the equilibrium weight at age, while discretizing integer age $a$ into $n_\Delta$ intervals, where fractional age $a^* = n_\Delta a + \Delta$ corresponds to interval $\Delta$ of integer age $a$:

$$\overline{\omega}_{a^*+1} = \overline{\omega}_{a^*} + \frac{H\overline{\omega}^d_{a^*}}{n_\Delta} - \frac{K\overline{\omega}_{a^*}}{n_\Delta} \tag{3}$$

We then assume that anabolism $\frac{H\omega^d_{a^*}}{n_\Delta}$ will vary with consumption, i.e.,:

1. If there is no consumption, then anabolism $\frac{H\omega^d_{a^*}}{n_\Delta}$ is zero, and individuals are predicted to shrink at rate $\frac{d}{dt}\omega = -K\omega$ with linear approximation $\omega_{a^*+1} = \omega_{a^*} - \frac{K\omega_{a^*}}{n_\Delta}$

2. If consumption, weight-at-age, and abundance-at-age are all at their equilibrium, then we expect growth to match its equilibrium value, and this occurs when anabolism is $\frac{H\overline{\omega}^d_{a^*}}{n_\Delta}$;

3. If consumption doubles relative to its equilibrium, we expect anabolism to also double.

As a further complication, a model might track consumption $Q$ only when aggregating across fractional ages. In the following, we partition fractional ages $a^*$ into "stanzas" (a.k.a. stages) $s2$, and model equilibrium consumption $\overline{Q}_{s2}$ (or other quantities) by summing across fractional ages $a^* \in s2$ within a given stanza $s2$. Alternatively, a model might aggregate all fractional ages $a^*$ into a stanza $s2$ representing a single integer age $a$, and track consumption $Q_a$ for each integer age.

To proceed, we rearrange the individual growth equation (Equation 3) to show that anabolism at equilibrium for fractional age $a^*$ is $\overline{\omega}_{a^*+1} - \overline{\omega}_{a^*} + \frac{K}{n_\Delta}\overline{\omega}_{a^*}$. Average individual anabolism must be supported by population-scale consumption $Q_{s2}$ for the corresponding stanza $s2$, and that stanza has metabolic demand $\sum_{a^* \in s2} v_{a^*}\omega^d_{a^*}$. At equilibrium, we therefore have an identity:

$$\overline{\alpha}_{a^*} \underbrace{\left(\frac{\overline{Q}_{s2}}{\sum\limits_{a^* \in s2} v_{a^*}\omega^d_{a^*}}\right)}_{\substack{\text{Equilibrium consumption} \\ \text{per biomass demand for stanza } s2}} = \underbrace{\overline{\omega}_{a^*+1} - \overline{\omega}_{a^*} + \frac{K}{n_\Delta}\overline{\omega}_{a^*}}_{\substack{\text{Equilibrium anabolism for} \\ \text{fractional age } a^*}}$$

$$\tag{4}$$

And solving for $\overline{\alpha}_{a^*} = \left(\overline{\omega}_{a^*+1} - \overline{\omega}_{a^*} + \frac{K}{n_\Delta}\overline{\omega}_{a^*}\right)\left(\overline{Q}_s / \sum_{a^* \in s2} \overline{v}_{a^*}\overline{\omega}_{a^*}^d\right)^{-1}$

then converts the ratio of consumption and metabolic demand for a given stanza $s2$ to anabolism for a given fractional age $a^*$. We can then use $\overline{\alpha}_{a^*}$ to calculate anabolism given other levels of consumption and metabolic demand:

$$\omega_{a^*+1} = \omega_{a^*} + \overline{\alpha}_{a^*}\frac{Q_{s2}}{\sum_{a^{*\prime} \in s2} v_{a^{*\prime}}\omega_{a^{*\prime}}^d} - \frac{K}{n_\Delta}\omega_{a^*} \quad (5)$$

This expression, therefore, links individual, age-specific growth increments to total consumption $Q_2$ aggregated over a set of fractional ages $a^* \in s2$. The expression satisfies our three objectives, i.e., (1) predicting a decline in body mass in the absence of consumption, with (2) weight-at-age matching equilibrium values given equilibrium age-structure and consumption, and (3) having a linear increase in anabolism with consumption. Future research could modify the third characteristic by shunting elevated consumption into elevated survival or reproductive output (Walters et al. 2000), although we do not explore this here.

In the following, we demonstrate how Equations (4) and (5) can be used to integrate bottom-up interactions into age-structured population dynamics. We specifically extend the state-space mass balance model Ecostate (and package *ecostate*), which predicts population growth rates based on both:

$$\underbrace{\overline{\beta}_i}_{\substack{\text{Equilibrium} \\ \text{biomass for prey } i}} \times \underbrace{p_i}_{\substack{\text{Prey} \\ \text{production} \\ \text{per biomass}}} \times \underbrace{e_i}_{\substack{\text{Prey} \\ \text{ecotrophic} \\ \text{efficiency}}} = \sum_{j=1}^{S}\left(\underbrace{d_{i,j}}_{\substack{\text{Proportion of} \\ \text{diet for predator} \\ j \text{ by prey } i}} \times \underbrace{\overline{\beta}_j}_{\substack{\text{Equilibrium} \\ \text{biomass for} \\ \text{predator } j}} \times \underbrace{w_j}_{\substack{\text{Predator} \\ \text{consumption} \\ \text{per biomass}}}\right) \quad (6)$$

1. *Theory*, i.e., heterotrophic species follow a simple biomass-dynamics model such that they have some assumed or estimated density dependence where, e.g., population growth rates will tend to increase as abundance declines (Figure S1);

2. *Observations*, i.e., where predicted biomass will closely match observed biomass indices when the latter are available, such that predicted dynamics are conditioned upon observations (i.e., population growth rates will increase or decrease to match observed trends in abundance).

In particular, we investigate whether having forage biomass indices can improve predicted changes in predator weight-at-age. However, future models could replace our density-dependent model for prey dynamics with user-specified indices of prey biomass or predator consumption (i.e., treating prey biomass or consumption as covariates).

## 2.2 | State-Space Mass Balance Modelling

Ecostate (Thorson et al. 2024) is a state-space model for population dynamics, which tracks biomass $\beta_s(t)$ for each $s \in \{1, 2, \ldots, S\}$ of $S$ functional groups in continuous time $t_{\min} < t < t_{\max}$. Functional groups are categorised as autotrophs (producers), heterotrophs (consumers), and detritus pools, and we index functional groups as prey $i$ and predator $j$ in expressions that involve predators and prey groups. It uses dynamical equations derived from Ecopath (Polovina 1984) and Ecosim (Walters et al. 1997, 2000; Christensen and Walters 2004) and extends these dynamics to permit: (1) any combination of parameters to be estimated via fit to time-series data using maximum likelihood, with options for likelihood penalties and/or Bayesian estimation; and (2) estimation of process errors representing unmodeled variation in dynamics, where the variance of process errors can be estimated as a hierarchical model. We first briefly summarise the previous development of Ecostate, before introducing how age-structured models are incorporated.

Ecostate (mimicking Ecopath) first defines an equilibrium biomass $\overline{\beta}_s$, where biomass inputs (primary production, assimilated consumption, and detrital inputs) match outputs (metabolic demand, biomass growth, natural mortality, predation mortality, and detrital turnover) on average for all functional groups. This equilibrium is expressed using the "master equation":

where $p_i$ is production per biomass, $e_i$ is the proportion of biomass that is utilised by modelled variables ("ecotrophic efficiency"), $d_{i,j}$ is diet proportions (where the diet matrix **D** has columns that sum to one for heterotrophs and zero otherwise), and $w_j$ is consumption per biomass. Fitting this equation requires that the analyst specify a fixed value (or estimate as fixed effect) for three of the four parameters $\{p_s, e_s, \overline{\beta}_s, w_s\}$ for each taxon, and such that the fourth value can be solved deterministically (Polovina 1984). We envision that analysts will typically solve for ecotrophic efficiency, although it could instead be estimated with a prior in cases when nearly all predators are being modelled.

Ecostate (mimicking Ecosim) then defines a differential equation for biomass dynamics over time $\beta_s(t)$ given these same parameters:

$$\frac{\mathrm{d}}{\mathrm{d}t}\beta_s(t) = \left( \underbrace{g_s(t)}_{\substack{\text{Growth} \\ \text{rate}}} - \underbrace{m_s(t)}_{\substack{\text{Natural} \\ \text{mortality} \\ \text{rate}}} - \underbrace{f_s(t)}_{\substack{\text{Fishing} \\ \text{mortality} \\ \text{rate}}} + \underbrace{\epsilon_s(t)}_{\substack{\text{Process error} \\ \text{in biomass rate}}} \right)\beta_{s,t}$$

(7)

$$\frac{\mathrm{d}}{\mathrm{d}t}\eta_s(t) = f_s(t)\beta_s(t)$$

where $g_s(t)$ is a population growth rate, $m_s(t)$ is the population mortality rate, $f_s(t)$ a fishing mortality rate, $\epsilon_s(t)$ is an optional process error in biomass rates, and $\eta_s(t)$ is an accumulator tracking fishery catches. Population growth $\mathbf{g}(t)$ and mortality $\mathbf{m}(t)$ are calculated based on a matrix of consumption rates, and see Table 1 for definitions. Biomass and catches across all groups are then integrated at an annual time step by default $(\boldsymbol{\beta}(t+1), \boldsymbol{\eta}(t+1)) = \int_t^{t+1}\frac{\mathrm{d}}{\mathrm{d}t}(\boldsymbol{\beta}(t), \boldsymbol{\eta}(t))$ numerically, e.g., using an Adams-Bashforth ordinary differential equation algorithm with user-specified accuracy (with other ODE solvers also available to users). The model can be fitted to a combination of biomass indices and fishery catch time-series (Thorson et al. 2024).

## 2.3 | Combining Age-Structured and Biomass Dynamics

Here, we extend Ecostate to incorporate age-structured dynamics for selected heterotrophs. This extension starts using the "multistanzas" functionality from Ecosim (Walters et al. 2000), but incorporates new options to:

1. Fit age-composition data, while weighting those data using a multinomial distribution with a known "input-sample size", or further down-weighting the input sample size using a Dirichlet-multinomial distribution as a diagnostic of model mis-specification (Thorson et al. 2023);

2. Fit empirical weight-at-age data;

3. Estimate logistic selectivity parameters via their fit to age-composition data;

4. Estimate parameters representing equilibrium weight-at-age, i.e., von Bertalanffy growth rate, asymptotic weight, the allometric scaling of consumption to size, and the proportion of animals that are mature for each age ("maturation ogive");

5. Estimate stock-recruit parameters representing equilibrium recruits and the steepness of the emergent stock-recruit relationship occurring at equilibrium conditions for other taxa;

6. Estimate annual variation in cohort strength beyond what's expected from the stock-recruit relationship as a random effect ("recruitment deviations"), while potentially

estimating the variance of recruitment deviations using maximum marginal or penalised likelihood;

7. Estimate annual variation in consumption for a given predator, beyond what is expected from the deterministic skeleton (Eq. T1.1).

These options have not previously been implemented in any model using Ecosim or extensions of the underlying equations. Collectively, these extensions allow us to use Ecostate to fit parameters for a full age-structured stock assessment model, including decadal projections, stock status, Bayesian priors, process errors, and model diagnostics. However, the age-structured model also incorporates both top-down (i.e., changes in natural mortality resulting from predator consumption) and bottom-up (i.e., changes in individual size resulting from consumption of prey) controls.

Following Ecosim, each age-structured population $g2$ is represented using one or more stanzas $s2[g2]$, and each stanza $s2$ is itself associated with a functional group $s[s2]$, such that the biomass for stanza-group of an age-structured population is $\beta_{s[s2[g2]]}$. To simplify presentation in the following, we discuss how age-structured dynamics are incorporated for a single age-structured population and suppress index $g2$ from notation throughout. However, the model (and associated code) is fully generic, and can incorporate age-structured dynamics for as many heterotrophs as specified by the user.

Stated briefly, Ecostate defines unfished equilibrium biomass $\frac{\mathrm{d}}{\mathrm{d}t}\overline{\beta}_s = 0$ for heterotroph $s$ as occurring when the population growth $\overline{g}_s$ (which arises from consumption) balances population mortality $\overline{m}_s$ (which arises from predation); mass balance for primary producers and detritus groups is detailed elsewhere (Thorson et al. 2024). To convert these biomass-dynamic rates to age-structured dynamics, Ecostate converts biomass mortality rate $m_s(t) + f_s(t)$ in Equation (7) to an individual mortality rate (which has no direct effect on somatic growth rates) and converts biomass growth $\overline{g}_s(t)$ to an individual growth rate (which has no direct effect on individual mortality rates). Both conversions are specified to satisfy two conditions at unfished equilibrium:

1. The conversion of equilibrium population mortality $\overline{m}_s(t)$ to individual mortality rate results in a stable age-distribution. Given weight-at-age and the stable age-distribution, we can calculate biomass-per-recruit for a given stanza $s2$, and equilibrium recruitment is calculated as biomass $\beta_{s[s2]}$ divided by biomass-per-recruit for that stanza $s2$. We then use equilibrium recruitment, stable age-distribution, and weight-at-age to calculate biomass for other stanzas. Equivalently, this equilibrium occurs when production per biomass $p_s$ for each stanza is equal to the mortality rate over the corresponding age range;

2. The conversion of the equilibrium population growth rate $\overline{g}_s(t)$ to individual growth results in a generalised von Bertalanffy growth function with a specified growth rate $k$, asymptotic weight $W_\infty$ and allometric scaling $d$. This condition is met by solving for equilibrium consumption and consumptive demand, and then applying Equations (4) and (5).

| Eq. | Description | Equations |
|---|---|---|
| T1.1 | Consumption rate | $c_{i,j}(t) = \underbrace{\overline{c}_{i,j}}_{\substack{\text{equilibrium} \\ \text{consumption rate}}} \times \underbrace{\dfrac{x_{i,j}^{\frac{\beta_j(t)}{\overline{\beta}_j}}}{x_{i,j}-1+\frac{\beta_j(t)}{\overline{\beta}_j}}}_{\substack{\text{predator functional} \\ \text{response}}} \times \underbrace{\dfrac{\beta_i(t)}{\overline{\beta}_i}}_{\substack{\text{prey functional} \\ \text{response}}}$ |
| T1.2 | Population mortality rate | $m_s(t) = \underbrace{\dfrac{\sum_{j=1}^{S} c_{s,j}(t)}{\beta_s(t)}}_{\text{Predation rate}} + \begin{cases} \underbrace{p_s(1-e_s)}_{\substack{\text{Residual natural} \\ \text{mortality rate}}} & \text{if } s \text{ is autotroph or heterotroph} \\ \underbrace{v_s}_{\text{Export rate}} & \text{if } s \text{ is detritus} \end{cases}$ |
| T1.3 | Detritus turnover rate | $\overline{\beta}_s v_s = \underbrace{\sum_{i=1}^{S}\sum_{j=1}^{S} u_j \overline{c}_{i,j}(t) + \sum_{j=1}^{S} \overline{\beta}_j p_s(1-e_s)}_{\text{Detritus accumulation}} - \underbrace{\sum_{j=1}^{S} \overline{c}_{s,j}(t)}_{\substack{\text{Detritus} \\ \text{consumption}}}$ |
| T1.4 | Population growth rate | $g_s(t) = \begin{cases} \dfrac{p_s}{w_s} \times \dfrac{\sum_{i=1}^{S} c_{i,s}(t)}{\beta_s(t)} & \text{if } s \text{ is heterotroph} \\ \dfrac{p_s \overline{\beta}_s}{\beta_s(t)} \times \dfrac{x_{s,s}^{\frac{\beta_s(t)}{\overline{\beta}_s}}}{x_{s,s}-1+\frac{\beta_s(t)}{\overline{\beta}_s}} & \text{if } s \text{ is autotroph} \\ \dfrac{\sum_{i=1}^{S}\sum_{j=1}^{S} u_j c_{i,j}(t) + \sum_{j=1}^{S} \beta_j(t) p_j(1-e_j)}{\beta_s(t)} & \text{if } s \text{ is detritus} \end{cases}$ |
| T1.5 | Measurement error for biomass index | $\log(b_s(t)) \sim \text{Normal}(\log(q_s \beta_s(t)), \sigma_s^2)$ |
| T1.6 | Measurement error for fishery catch | $\log(h_s(t)) \sim \text{Normal}(\log(\eta_s(t)), v_s^2)$ |
| T1.7 | Process error for biomass rates | $\epsilon_s(t) \sim \text{Normal}(0, \tau_s^2)$ |

*Note:* Note that Equation T1.1 is replaced when estimating annual variation in consumption.

Further details are provided in Appendix S1.

## 2.4 | Fitting to Data

In particular, we calculate the likelihood of age-composition data **N** containing vector $\mathbf{n}_t$ of samples $n_{a,t}$ for each integer age $a$ in year $t$. However, age-composition sampling typically arises from a monitoring program with some selectivity-at-age $s_a$, so we estimate two parameters $\theta_1$ and $\theta_2$ that represent the logistic survey selectivity, $s_a = \left(1 + e^{\theta_1 - \frac{a}{\theta_2}}\right)^{-1}$:

$$\mathbf{n}_t \sim \text{Multinomial}\left(\frac{\mathbf{s}\boldsymbol{\nu}(t)}{\sum_{a=1}^{a_{\max}} s_a v_a(t)}\right)$$

where $\sum_{a=1}^{a_{\max}} n_a(t)$ is the input sample size which determines the weighting of these data relative to other information. Alternatively, we can instead specify a "linear" Dirichlet-multinomial distribution:

$$\mathbf{n}_t \sim DM\left(\frac{\mathbf{s}\boldsymbol{\nu}(t)}{\sum_{a=1}^{a_{\max}} s_a v_a(t)}, \theta_3\right)$$

where $\theta_3$ is (approximately) the ratio of input and effective sample size (Thorson et al. 2017).

Similarly, we calculate the likelihood of empirical weight-at-age data **W** containing the average body weight $w_{a,t}$ for each integer age and year. We specify a lognormal distribution:

$$\log(w_{a,t}) \sim \text{Normal}\left(\log(\omega_a(t)), \sigma_w^2\right)$$

where $\sigma_w^2$ is an estimated parameter representing the residual variance in weight-at-age data (and future research could incorporate sampling variability as an additional variance when fitting weight-at-age data). Model exploration suggests that age-composition data are informative about production-per-biomass $p_{s2}$ (which is proportional to natural mortality rate), and that weight-at-age data are informative about the von Bertalanffy growth parameters $k_{g2}$ and $d_{g2}$.

Finally, we include options to estimate unexplained variation in age-structured dynamics:

1. *Recruitment deviations*: We estimate an annual "recruitment deviation" $\phi(t)$ which is assigned a normal distribution:

$$\phi(t) \sim \text{Normal}\left(0, \sigma_\phi^2\right)$$

where $\sigma_\phi^2$ is the variance of recruitment deviations, and can either be estimated using maximum marginal likelihood or fixed a priori when using penalised likelihood estimates. Recruitment deviations can then be informed by unexplained variation in age-composition data. Recruitment deviations will arise because cohort strength is strongly influenced by small differences in daily rates of larval survival resulting from ocean temperatures and advective fields (Cushing 1990), which may be largely independent of trophic interactions represented within Ecostate.

2. *Consumption deviations*: Similarly, variation in oceanographic conditions (e.g., temperature) may drive variation in predator–prey overlap and/or predator metabolic demand. We therefore incorporate annual variation in predator consumption, where we replace the deterministic equation for consumption (Eq. T1.1) from Ecostate with a "semi-parametric" equation:

$$c_{i,j}(t) = \underbrace{\overline{c}_{i,j}}_{\substack{\text{equilibrium} \\ \text{consumption rate}}} \times \underbrace{\frac{x_{i,j} \frac{\beta_j(t)}{\overline{\beta}_j}}{x_{i,j} - 1 + \frac{\beta_j(t)}{\overline{\beta}_j}}}_{\substack{\text{predator functional} \\ \text{response}}} \times \underbrace{\frac{\beta_i(t)}{\overline{\beta}_i}}_{\substack{\text{prey functional} \\ \text{response}}} \times e^{\nu_j(t)}$$

where we again assign a normal distribution to consumption deviations:

$$\nu_j(t) \sim \text{Normal}\left(0, \sigma_{\nu,j}^2\right)$$

where this magnitude of variation can again be either estimated or fixed a priori, depending upon computational constraints. An increase in consumption then decreases survival for prey species and increases weight gain for the predator. Annual variation in consumption can therefore be informed either via unexplained variation in prey biomass and/or predator weight-at-age.

3. *Survival deviations*: We note that process errors can be estimated for the biomass of any functional group, and this includes stanza of age-structured populations. Ecostate is parameterised

such that process errors result in unexplained variation in survival rates when applied to age-structured groups. These process errors can then represent either excess mortality or immigration/emigration, similar to their interpretation in state-space age-structured models (Stock et al. 2021).

## 2.5 | Parameter Estimation

Building upon the mass-balance model Ecostate, we continue to estimate parameters using RTMB (Kristensen 2024). This then provides a user-friendly interface to automatic differentiation (AD) and the Laplace approximation provided by TMB (Kristensen 2014). However, age-structured calculations in Ecostate involve large matrices of abundance-at-age and weight-at-age for fractional ages $a^*$ and years $t^*$. Given the size of the AD tape, it is not feasible to repeatedly calculate the Hessian matrix as required when using the Laplace approximation to apply maximum marginal likelihood. We therefore optimise the penalised likelihood while fixing the variance of random effects at values that are specified a priori. Future research could estimate these parameters via a hierarchical Bayesian model, i.e., using tmbstan (Monnahan and Kristensen 2018) to sample the joint likelihood, but we do not explore the topic further here.

## 2.6 | Case Study Demonstration

To demonstrate, we fit the model to age-structured survey data for two commercially important species (walleye pollock and sablefish) as well as their primary energetic pathways (i.e., zooplankton, benthic invertebrate fauna, primary producers, and benthic detritus) in the Gulf of Alaska. These data include:

1. Survey data for pollock from a stratified random bottom-trawl survey conducted biennially from 1990 to 2023 by the AFSC (Siple et al. 2024). Design-based estimators are used to generate a biomass index, age composition (in numbers, excluding 2023), and average weight-at-age. Survey data east of 140 W are excluded as there is evidence that it is a separate stock. Total catches from 1970 to 2023 were also fitted, and details about how they were obtained can be found in Monnahan et al. (2023).

2. Survey data from a longline survey for sablefish, which follows a systematic survey design, including age-composition (in numbers), empirical weight-at-age, and a biomass index (in mass). We reprocessed the data to only include sets in the Gulf of Alaska, i.e., excluding stations occurring in the Bering Sea or Aleutian Islands. Given the unknown area of attraction for longline gear, the biomass index is calculated using a depth-stratified, area-weighted estimator, and the biomass time-series is treated as a relative index (i.e., estimating a catchability coefficient).

3. Total annual fishery harvest for the two directed fisheries, extracted from the most recent stock assessments for pollock (Monnahan et al. 2023) and sablefish (Goethel et al. 2024);

4. An Rpath model for the Western Gulf of Alaska, where we use annual biomass production per biomass $p_s$, annual consumption per biomass $w_s$ (which includes digested and

unassimilated consumption in biomass), and the diet proportions matrix $d_{i,j}$, as well as equilibrium biomass $\bar{\beta}_s$ for those species where Ecostate is unable to estimate this based on available information.

5. A biomass index for large copepods from the EcoFOCI survey; Large copepod (> 2 mm; example species: *Calanus* spp. and *Neocalanus* spp.) abundance (numbers per cubic meter) was estimated from 505 μm mesh, 60 cm diameter bongo nets. Total large copepod abundance is summed for each station sampled within two core areas, one in spring and one in summer, and the mean abundance is calculated from all stations within the core areas (Kimmel et al. 2023).

6. A biomass index for euphausiids from the Seward Line (Hopcroft 2023).

We note that the sablefish stock assessment includes data from the Gulf of Alaska, Bering Sea, and Aleutian Islands; therefore, it does not exactly match our spatial scale (which is restricted to the Gulf of Alaska). Similarly, the pollock assessment uses a somewhat restricted spatial scale that excludes southeast Alaska. We instead use the spatial scale of the Rpath model for the Western Gulf of Alaska and expect that the difference in spatial scale will produce some differences in model results relative to estimates from each stock assessment.

For each age-structured population, we estimate unfished biomass for juveniles and adults (four scale parameters; Table 2). We also estimate the catchability coefficient and two logistic selectivity parameters for the primary survey of each species. To match the pollock stock assessment, we specify a lognormal likelihood penalty on the bottom-trawl survey catchability for pollock, with log-mean of log(0.85) and log-standard deviation of 0.1. To match the two stock assessments, we fix steepness $h = 0.999$ (i.e., approaching a constant stock-recruit relationship) and estimate recruitment deviations $\phi_s(t)$. We encourage future research exploring the impact of estimating steepness (presumably using a prior distribution), but to not explore it here. For both sablefish and pollock, we assumed that the input-sample size for age-composition data was 60 in each year, and used the Dirichlet-multinomial likelihood to weight these data. However, the effective sample size approached the input value (60) for both species, such that we then reverted to nominal weighting using the multinomial likelihood. We also fix age-at-maturity $a_{mat} = 6$ for sablefish and $a_{mat} = 4$ with logistic slope $w_{matslope} = 1$ to (approximately) match the sablefish and pollock assessments, and fix juvenile natural mortality at values from the Rpath model ($M = 1.65$ and $1.96$ for sablefish and pollock, respectively). We estimate adult natural mortality rate for each age-structured species, while specifying a likelihood penalty centred on the value assumed in the stock assessment (sablefish: 0.1; pollock: 0.30) and with a log-standard deviation of 0.1. We specify specialised von Bertalanffy growth rate $k = 0.14$ for sablefish and $k = 0.2$ for pollock, and specify allometric consumption $d = \frac{1}{2}$ for sablefish and $d = \frac{2}{3}$ for pollock. These are fixed here (because we are withholding weight-at-age data for model evaluation), but model exploration suggests that they are estimable when fitting to weight-at-age data.

**TABLE 2** | List of estimated parameters for the two age-structured populations (sablefish and walleye pollock) in the Gulf of Alaska case study, where juveniles are ages [0–2] and adults are ages [2, 15+] for pollock and [2, 31+] for sablefish, where equilibrium values refer to unfished equilibrium.

| Parameter | Ecostate estimate (standard error) | | Stock assessments | |
| --- | --- | --- | --- | --- |
| | **Sablefish** | **Pollock** | **Sablefish** | **Pollock** |
| Equilibrium juvenile biomass (million tons) | 0.014 (0.003) | 0.192 (0.059) | — | 0.252 |
| Equilibrium adult biomass (million tons) | 0.361 (0.049) | 1.609 (0.415) | 0.716 | 2.333 |
| Equilibrium juvenile natural mortality rate (year$^{-1}$) | 1.65 | 1.96 | — | 1.39 |
| Equilibrium adult natural mortality rate (year$^{-1}$) | 0.095 (0.029) | 0.408 (0.106) | 0.114 | 0.3 |
| Equilibrium juvenile trophic level (unitless) | 3.563 (< 0.001) | 3.55 (< 0.001) | — | — |
| Equilibrium adult trophic level (unitless) | 4.164 (< 0.001) | 3.594 (< 0.001) | — | — |
| Steepness (unitless) | 0.999 | 0.999 | 1 | 1 |
| Equilibrium age at maturity (year) | 6 | 4 | 7 | 4.742 |
| Equilibrium von Bertalanffy growth (year$^{-1}$) | 0.14 | 0.2 | 0.202 | — |
| Allometric consumption by weight (unitless) | 0.5 | 0.667 | — | — |
| Catchability coefficient (unitless) | 10.191 (3.226) | 1.025 (0.312) | 6.359 | 0.800 |
| Age at 50% survey selectivity (year) | 3.917 (0.09) | 5.944 (0.42) | 3.004 | 4.00 |
| Slope for logistic survey selectivity (year$^{-1}$) | 0.559 (0.042) | 1.365 (0.08) | 2.418 | 0.637 |
| Vulnerability $x_{ij} = x_j$ for predator $j$ (unitless) | 1.595 (0.362) | 3.259 (1.334) | — | — |

*Note:* For estimated parameters, we show the estimate with standard error in parentheses (note that the standard error for predicted trophic level is small because forage species have biomass that is fixed at Rpath values). For values fixed a priori, we show the fixed value without standard error. The age at 50% maturity for walleye pollock is calculated as an average from 1983 to 2023 based on annual regression estimates (see fig 1.18 of Monnahan et al. (2023) for original data). Uncertainty about equilibrium biomass is not typically calculated for these age-structured stock assessments and is not included here. Pollock age maturity from the stock assessment is calculated as the average of an annual value; other values for assessment are listed as "–" when not available.

To represent species interactions, we estimate a vulnerability parameter $x_{ij} = x_j$ representing the constant vulnerability all prey $i$ for each of sablefish or pollock as predators $j$ (Table 2), and specify a lognormal penalty on vulnerability $x_j$ with log-mean log(2) and log-standard deviation of 1.0 (where 2 is the default value used in most Ecosim implementations). In addition, we estimate the catchability coefficient for large copepods and euphausiids (such that estimated biomass will tend to match the assumed equilibrium biomass fixed from Rpath), and estimate process-errors $\epsilon_s(t)$ for biomass dynamics of copepods and euphausiids (to allow the model to match observed cycles and trends for zooplankton forage). Given that we are using penalised likelihood (to avoid the computational cost of computing the Laplace approximation), we fix the variance of recruitment deviations (i.e., $\sigma_\phi^2 = 1^2$ for both case study species) and fix the variance of process errors for copepods and euphausiids (i.e., $\sigma_\epsilon^2 = 1^2$ for both). However, we confirm that the average across years of the standard-error squared and the sample variance for deviations approximately matches the input variance (i.e., the tuning metric discussed in Methot and Taylor (2011)).

To evaluate model performance, we explore six assessments of model performance:

1. *Convergence*: We confirm that the model is converged; i.e., it has a small gradient of the negative log-likelihood with respect to parameters $< 0.001$ and a positive-definite Hessian matrix;

2. *In-sample fit*: We fit to age-composition data and biomass indices and visually compare the predicted and observed values for these data. This comparison is widely used when reviewing stock-assessment and ecosystem models (e.g., a Level-1 metric from Hipsey et al. 2020);

3. *Consistency with stock assessments*: We compare model estimates (and standard errors) with estimates from single-species stock assessments for pollock (Monnahan et al. 2023) and sablefish (Goethel et al. 2024);

4. *Leave-future-out cross-validation*: We conduct a retrospective experiment where we fit data through year $T$, and exclude all biomass index and age-composition data in forecasted years from $T + 1$ through 2040. However, we retain data for fishery catches in all years (including forecasted years), so that biomass is forecasted given the observed fishery harvest. We fit 10 "retrospective peels" where the year of last data $T = \{2022, 2021, \ldots, 2013\}$, and record the forecast (and standard error) for biomass and recruitment deviations $\epsilon_t$ for pollock and sablefish. We visually compare these forecasts and standard errors with the estimates arising when fitting to all data ($T = 2023$);

5. *Predictive performance for weight-at-age*: We do not fit weight-at-age data directly. Instead, we use the model to predict annual weight-at-age and then compare these predictions with out-of-sample weight-at-age measurements. We explore this comparison visually, and also calculate the Pearson correlation between log-prediction and log-measurement for each age separately and then average this correlation across ages. We also evaluate predictive performance (#4 above) by comparing predicted weight-at-age

against a smoothed version of measured weight-at-age, estimated using a state-space model that includes age, year, and cohort effects (Cheng et al. 2024). This state-space model is intended to filter out measurement error in the observed weight-at-age (resulting from low but known sample sizes) prior to the comparison with predictions from Ecostate.

6. *Value of zooplankton surveys*: We compare the base model with an alternative scenario where we exclude biomass indices for zooplankton forage (euphausiids and copepods). This requires eliminating the catchability coefficient for these indices as well as process-error deviations for these taxa. We then visually examine how this changes estimates of biomass trends for all taxa, as well as its impact on the out-of-sample predictions for weight-at-age for sablefish and pollock.

Carvalho et al. (2021) claimed that a stock-assessment model is suitable for management if (a) it optimises successfully, (b) fits well to data, (c) provides reliable estimates of population scale and trend, (d) produces consistent results with new data, and (e) can provide adequate estimates of future states (e.g., during leave-future-out cross validation). Criterion (a) corresponds to our metric #1, (b) corresponds to #2, (c) corresponds to #3, and (d-e) corresponds to #4. We therefore believe that metrics #1–4 provide a proof-of-concept for how Ecostate could be reviewed for operational use in management. Meanwhile, #5 is only feasible given that we include bottom-up interactions to explain weight-at-age, and this is not a standard model-skill metric for stock assessment. Similarly, #6 is intended to illustrate the value of including prey information in stock assessment.

Collectively, the model estimates population scale for the two age-structured populations while tracking cohorts, and predicts time-varying natural mortality (from cannibalism and predation) and growth (from consumption and weight-specific metabolism). We can therefore view the model from two perspectives: as a stock-assessment model with two age-structured populations, and as a mass-balance model with species interactions. We therefore organise the Results to highlight these two perspectives.

## 3 | Results

### 3.1 | Stock Assessment Model With Age-Structured Dynamics

Inspecting model output from a stock-assessment perspective, we see clear evidence in the age composition for sablefish (Figure 1) of a strong cohort born in 1997 (showing up at age-4 in 2001), 2005 (showing up at age-5 in 2009), and again in 2014 and 2016 (showing up at age-3 in 2017 and 2019). As expected, these cohorts result in increasing biomass as they grow through the population, i.e., from 2001 to 2003, 2008 to 2010, and again from 2017 to 2023 (Figure 2). These latter cohorts result in adult sablefish biomass in 2023 approaching a high last seen at the beginning of biomass index data (1990). However, biomass relative to the equilibrium unfished level is still expected to increase over subsequent years towards the unfished equilibrium (Figure S2) under the scenario projected here (i.e., no catches after 2023).
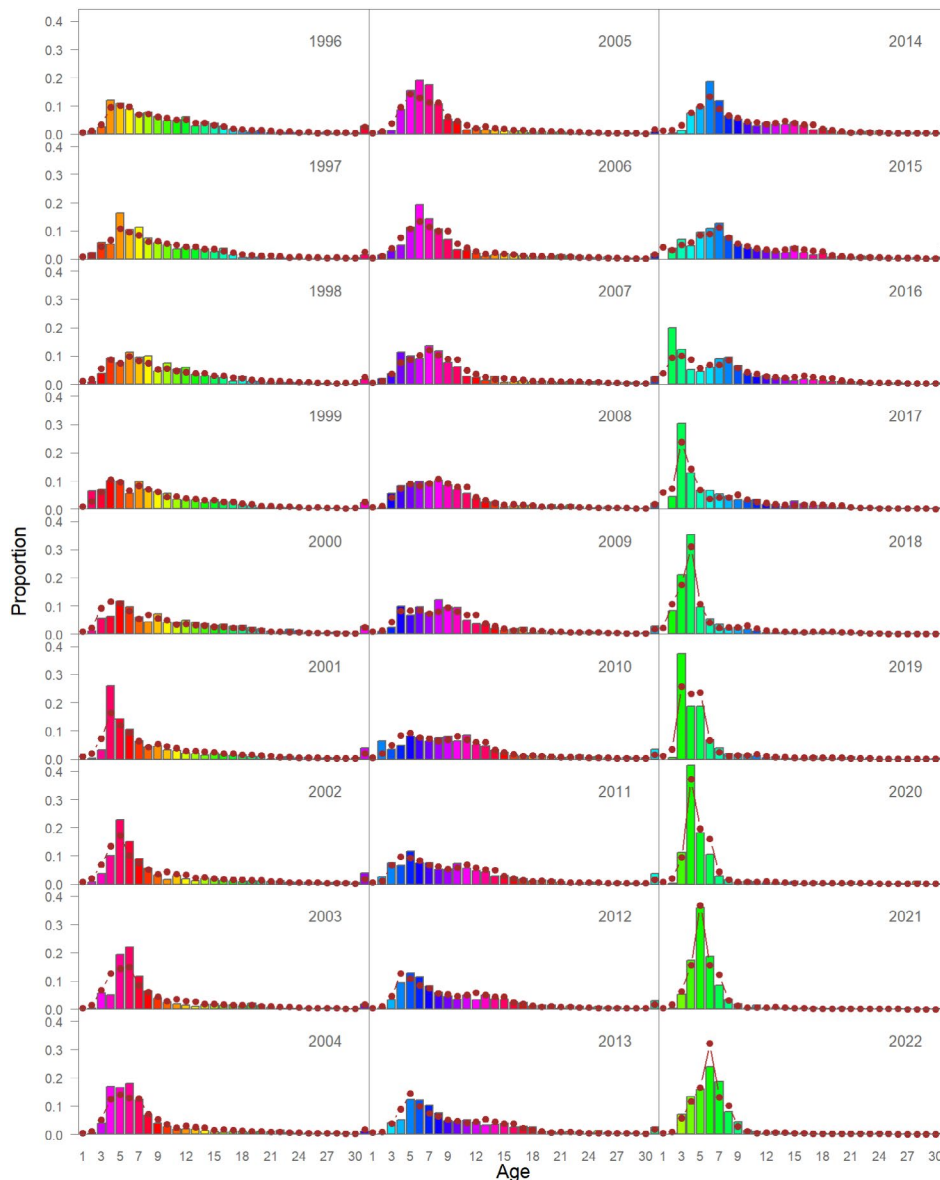
**FIGURE 1** | Proportion at age (*y*-axis) for ages 1–31+ (*x*-axis) for sablefish in each year with available age-composition data (panels), showing measurements (coloured histograms) and estimated value (red dots and lines), where estimates are the product of predicted abundance-at-age $v_{g2}(t)$ and selectivity-at-age. Bars are colour-coded to have a single colour for a given cohort across years, to facilitate tracking cohorts across years. Note that the data are for ages 2–31+ (hence no bar for age-1), whereas the model predicts for ages 1–30+.

Similarly, inspecting survey age-composition for walleye pollock (Figure 3), we see strong cohorts in 1988 (showing up at age-2 in 1990 and age-5 in 1993), 2000 (ages 1/3/5/7 in 2001 onward), 2004 (ages 1/3/5 starting in 2005) and 2012 (showing up at ages 1/3/5), and these allow the predicted and observed abundance-at-age to closely match. Finally, there is preliminary information about important cohorts in 2016 and 2020, which show up at ages 1 and later despite the continuing size of the 2012 cohort. The 2000 cohort is associated with rapid increases in adult biomass from 2001 to 2003, and the 2004 cohort causes an increase from 2006 to 2009 (Figure 3). Finally, the strong recent cohorts have driven an estimated increase from 300 to over 1000 kt from 2020 to 2023. Under a scenario of no future fishing, pollock biomass is then expected to decline slightly towards its unfished equilibrium (Figure S2).

## 3.2 | Mass-Balance Model With Species Interactions

Inspecting model output from a mass-balance model perspective (Figure 4), we see that adult sablefish has an equilibrium trophic level (TL) of 4.1 due to consuming adult pollock (TL: 3.6), while juveniles of both species have similar trophic positions (TL: 3.6; see Table 2). As expected, given this higher TL, adult sablefish has a lower natural mortality rate (0.10) than adult pollock (0.41) and also has a lower total biomass (adult sablefish: 361 kt; adult pollock: 1609 kt).

The model estimates process errors in biomass dynamics for euphausiids and large copepods, which result in estimated biomass that closely matches available biomass-index data
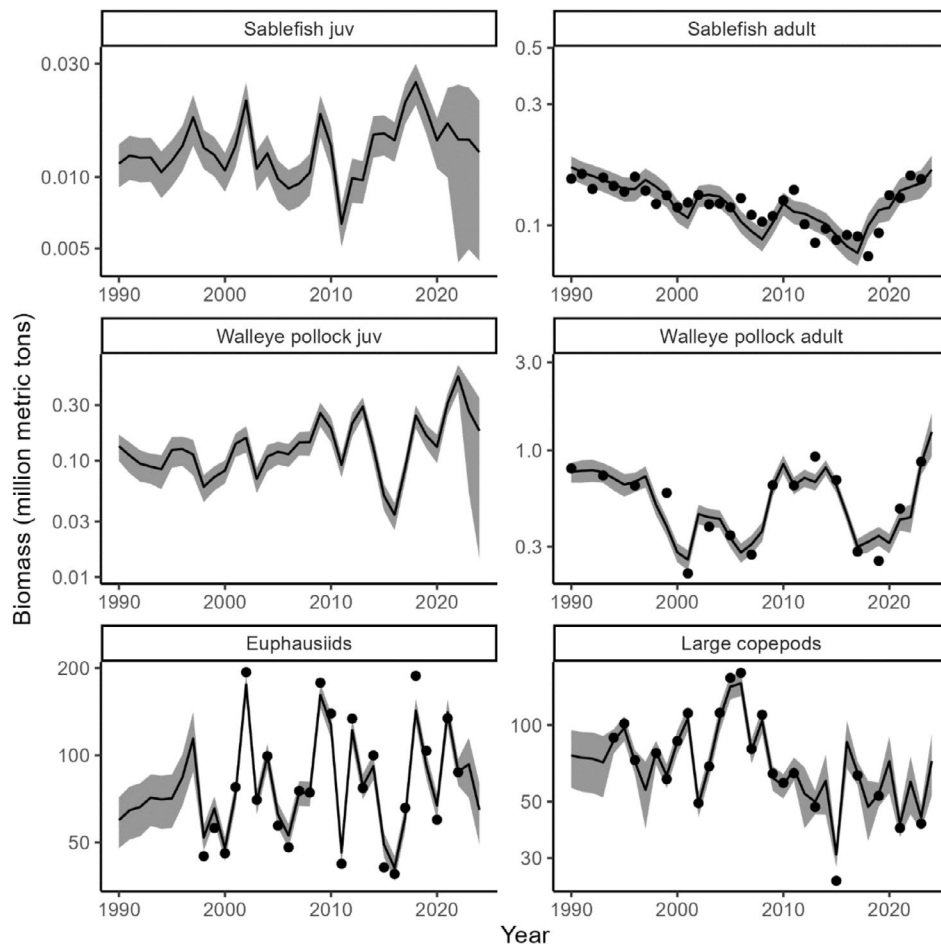
**FIGURE 2** | Estimated biomass (*y*-axis in million tons, with log-scale axis) in each year (*x*-axis) with available biomass-index data (1990–2023) and for the six functional groups that are affected by biomass indices (panels), showing observed values divided by the estimated catchability coefficient (dots) as well as the estimated value (black line) ±1.96 standard errors (shaded polygon).

(Figure 2). It then predicts interannual variation in zooplankton consumption and resulting weight-at-age for pollock and sablefish (Figure 5 top row). Euphausiids are predicted to have cyclic variation in biomass with highs in 2002, 2009, and 2018, with both highs and lows generally decreasing over that period. By contrast, large copepods are predicted to decline consistently from 2005 to 2015 before subsequently stabilising (Figure 2).

## 3.3 | Model Assessment #1: Convergence

The model has a minimal (< 0.001) gradient of the negative log-likelihood with respect to each parameter, and has a positive definite Hessian. We also confirm that it is numerically stable by confirming that it estimates the same parameters from different starting values for parameters, and is also insensitive to small changes in the temporal step-sizes used in the Euler or Adams–Bashforth algorithms for age-structured and biomass dynamics, respectively.

## 3.4 | Model Assessment #2: In-Sample Fit to Age-Composition Data

As expected, estimating recruitment deviations for pollock and sablefish allows the model to track strong cohorts over

time. This in turn allows the model to predict abundance-at-age that closely matches observed values (i.e., bar heights match points in Figures 1 and 3). However, this "in-sample" fit does not say anything about performance beyond the range of data, so we next explore "out-of-sample" predictive performance.

## 3.5 | Model Assessment #3: Comparison With Stock Assessments

Comparing estimated equilibrium biomass for adults (ages 2+) with values from recent stock assessments (Table 2), we see that Ecostate estimates somewhat lower total adult biomass than each stock assessment. For sablefish, this likely arises because Ecostate is fitted to a smaller spatial domain than the original stock assessment. Ecostate then compensates for this lower biomass estimate by estimating a higher value for the survey catchability coefficient for both species. By contrast, the estimated equilibrium natural mortality is lower for sablefish and higher for pollock than the corresponding stock assessment. Finally, the age at 50% survey selectivity is somewhat higher for Ecostate than the corresponding stock assessment, presumably because Ecostate has declining natural mortality with size (and therefore higher abundance at lower
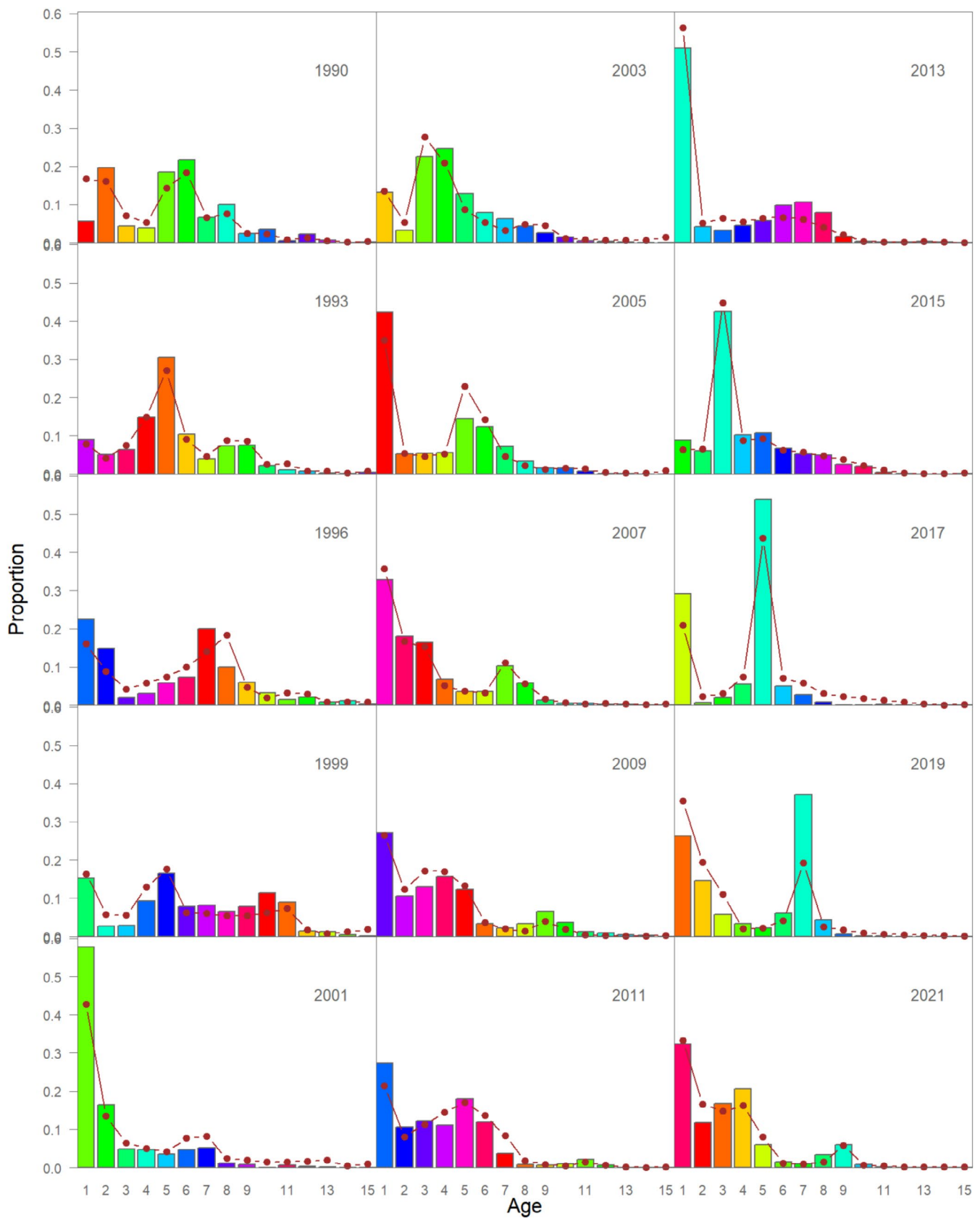
**FIGURE 3** | Proportion at age (*y*-axis) for ages 1–15+ (*x*-axis) for walleye pollock in each year with available age-composition data. Bars are colour-coded to have a single colour for a given cohort across years, to facilitate comparison across years (see Figure 1 caption for more details).
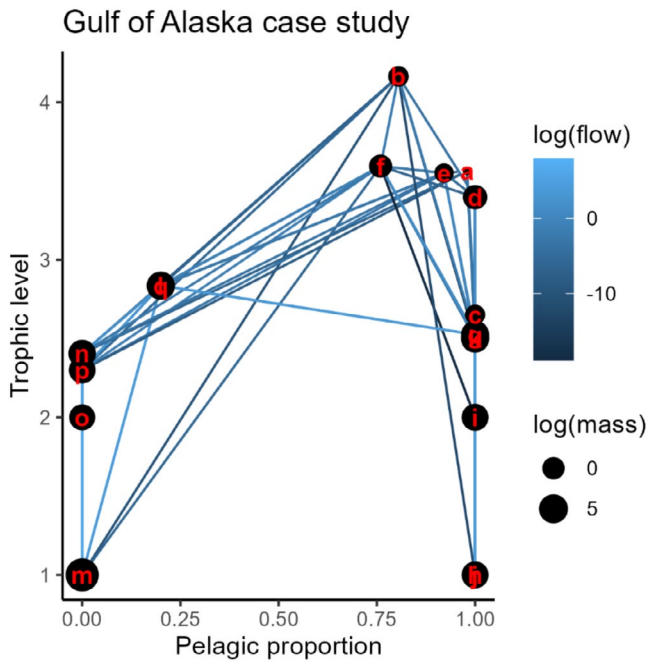
**FIGURE 4** | Estimated food web at equilibrium, with each taxon plotted according to its estimated proportion of pelagic production (*x*-axis) and trophic level (*y*-axis), with bullet size proportional to log-mass (in units million metric tons), and with edges colour-coded based on log-carbon flow (in units million metric tons per year). We show juvenile and adult sablefish (a and b), large microzooplankton (c), gelatinous carnivores (d), juvenile and adult pollock (e and f), euphausiids (g), large zooplankton (h), small microzooplankton (i), small phytoplankton (j), large copepods (k), pandalid shrimp (l), benthic detritus (m), infauna (n), benthic microbes (o), benthic zooplanknton (p) and non-pandalic shrimp (q) (i.e., same order as panels in Figure S2).

ages all else equal), whereas the stock assessments have constant natural mortality at age.

### 3.6 | Model Assessment #4: Leave-Future-Out Cross-Validation

We conduct a retrospective experiment removing data, forecasting dynamics under future catches, and comparing forecasts with subsequent predictions when fitting all data (Figure 6). The model has information to precisely estimate recruitment deviations $\phi(t)$ for sablefish three to four years after a given year-class (e.g., the 2019 year-class has stabilised using data through 2022 or 2023), whereas for pollock it estimates them two to three years after (e.g., the 2019 year-class has stabilised by 2021) and there is preliminary evidence in 2023 data of a strong year-class in 2021.

These retrospective estimates of year-class strength then propagate forward during biomass forecasts. Forecasted biomass is generally within the 95% confidence interval, even when removing 10 years of data; however, 10-year forecasts of adult pollock biomass range from essentially zero to twice the unfished equilibrium value (Figure 6 1st and 2nd rows). Sablefish biomass has increased faster from 2020 onward than what was expected using data available in 2020 (which did not have information
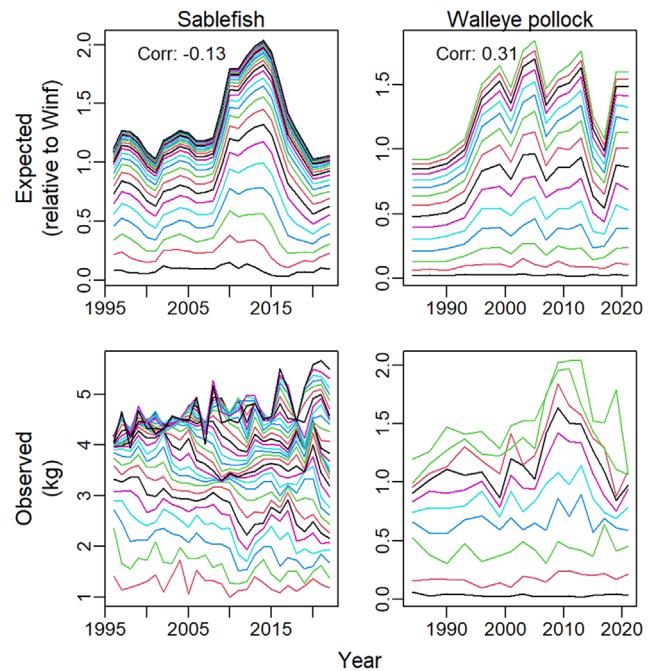


**FIGURE 5** | Comparison of predicted weight-at-age (top row) and withheld measurements that are not fitted (bottom row) for walleye pollock (left column) and sablefish (right column), showing the weight (*y*-axis) relative to equilibrium for the expected value or in KG for the observed value for each year with available data (*x*-axis). We compute the Spearman correlation over time for each age, and then the average correlation across ages for each species and list that value in the top panels.

about higher-than-average recruitment after 2016, Figure 6 3rd row). Similarly, adult pollock biomass forecasts have very broad confidence intervals when forecasting 6+ years forward, and recent biomass in 2020–2023 is lower than expected in 2013–2015 (Figure 6 2nd row) due to lower-than-average recruitment from 2013 to 2020 (Figure 6 4th row).

### 3.7 | Skill Assessment #5: Out-Of-Sample Weight-At-Age Predictions

Adult pollock weight-at-age is predicted to increase from 1993 to 2002 and then decline from 2002 to 2015 (Figure 5 top-right panel). This increase and subsequent decrease in adult pollock weight-at-age is attributed to the increase and subsequent decline in euphausiid abundance, associated pollock consumption and resulting weight-at-age (Figure S3). Following 2016, adult pollock are then predicted to have increasing weight-at-age, associated with an increase in adult pollock cannibalism resulting from the strong 2011 cohort (Figure S3 bottom-right panel). These predicted patterns in log-weight-at-age have a moderate (0.31) Pearson correlation with held-out survey measurements of log-weight-at-age, which show a progressive increase from 1993 to 2002 but also a later peak in 2008–2012, and no evidence of an increase in 2018 onward (Figure 5 bottom-right panel).

Similarly, the model predicts a peak in adult sablefish weight-at-age in 2014 (when adult sablefish is approaching its lowest levels), and a subsequent drop below equilibrium
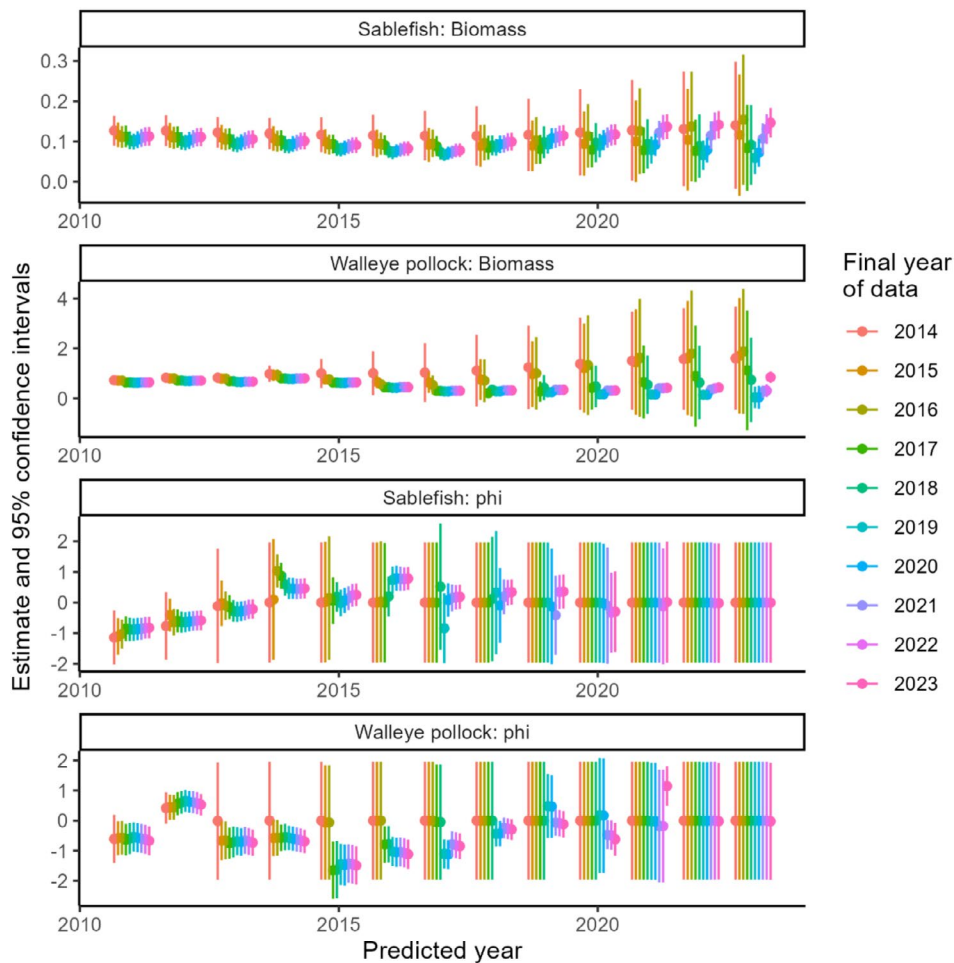
**FIGURE 6** | Retrospective peels for sablefish biomass (top row), pollock biomass (2nd row), sablefish recruitment deviation $\phi(t)$ (3rd row) or pollock recruitment deviation $\phi(t)$ (4th row) showing estimated values (*y*-axis) for 2011–2023 (*x*-axis) using data through 2023 (i.e., all data), 2022, 2021, ..., or 2013, i.e., for ten retrospective peels (see colour bar on right-hand side), showing the dot (line) and 95% confidence interval ($\pm$1.96 standard errors, whiskers) for each run.

weight-at-age (Figure 5 top-left panel). These predictions have a weakly negative (−0.13) correlation with held-out measurements of weight-at-age, which show declines for ages 2–10 and increases for the oldest ages (Figure 5 bottom-left panel). The correlation between predictions and out-of-sample data is largely unchanged for pollock when comparing against smoothed measurements, but is somewhat more negative for sablefish (Figure S4).

## 3.8 | Skill Assessment #6: Value of Zooplankton Indices

When we remove indices for copepods and euphausiids, predicted euphausiid biomass then has a strong negative correlation with adult pollock biomass, and copepods have a strong positive correlation (Figure S5), which contrasts strongly with the model predictions when fitting indices for these zooplankton species (Figure 2). Predicted patterns in weight-at-age for sablefish and pollock are then different due to changes in predicted consumption of large copepods and euphausiids, and the correlations between predicted and observed weight-at-age decline for both fishes (Figure S6).

## 4 | Discussion

In this paper, we summarise a generic method to incorporate bottom-up interactions in age-structured population models, which calculates individual growth rates from population-level consumption relative to metabolic demand. This method uses a minimum of additional information, i.e., weight-at-age and consumption in a reference time and variable consumption used to calculate growth increments during other times. It could therefore be repurposed in other models as long as prey forage and/or consumption is modelled or specified as a covariate. We then integrate the method into a recent state-space mass balance model, Ecostate and use modern statistical computing (e.g., automatic differentiation) to efficiently estimate both demographic rates (e.g., equilibrium recruitment), measurement parameters (e.g., catchability coefficients and survey selectivity-at-age) and process errors (e.g., recruitment deviations) using penalised likelihood estimation. In our case study, we showed that Ecostate can fit biomass and age-composition data for multiple age-structured species, and that fitting to forage biomass indices improves out-of-sample predictions of predator weight-at-age. This represents the first (to our knowledge) effort to combine state-space age-structured

modelling with multispecies modelling that includes both top-down and bottom-up interactions, and the resulting model can be viewed as both a stock-assessment and a mass-balance ecosystem analysis.

We recommend that models used to inform fisheries management be extended to link individual size-at-age to population-level consumption, whether using a full density-dependent model for prey populations (as we do here) or using indices of prey abundance or resulting consumption. We recommend this for two reasons:

1. *Climate forecasting*: many hypothesised mechanisms linking climate to population-level productivity depend upon forage availability. For example, increased temperature will cause an increase in metabolic demand; this could increase population growth rates if the predator can compensate via increased consumption. However, increased temperature could instead cause starvation in instances when sufficient prey forage is not available. Therefore, bottom-up interactions are likely important when developing climate-enhanced stock assessments;

2. *Weight-at-age forecasting*: harvest forecasts are sensitive to assumptions about future changes in weight-at-age. Linking weight-at-age to consumption provides a novel and mechanistic basis for forecasting weight-at-age for use in harvest control rules.

However, these efforts are presumably only useful when consumption can predict weight-at-age, e.g., for pollock but not sablefish in the case study here.

Ecostate could be used operationally to estimate stock status and forecast future biomass under alternative management or climate scenarios. We envision that Ecostate could pass regional review standards for use in tactical fisheries management, joining the small list of other examples (Bentley et al. 2021; Chagaris et al. 2020). For this reason, we provided a proof-of-concept for how Ecostate could be evaluated using the five diagnostic steps suggested for reviewing stock assessment (Carvalho et al. 2021). To facilitate further simulation testing, we have also provided Ecostate as a fully-documented R-package on CRAN, and this simulation testing would presumably be needed for any future review for management use (Kapur et al. 2025). However, we ultimately believe that stakeholders will be more receptive if existing models are augmented to link individual size-at-age to population-level consumption, rather than adopting entirely new software and methods. For this reason, we have focused our presentation on the theory and methods (Equations 1–5) that could be repurposed in other models that are already being used to inform management.

Our analysis links individual growth to population-scale consumption by adapting a differential equation for growth based on anabolism and catabolism (Equation 1). However, Von Bertalanffy (1960) additionally hypothesised that (1) both anabolism rate $H$ and catabolism rate $K$ would increase with temperature and (2) anabolism would increase with temperature faster than catabolism. The first hypothesis is widely supported (Kingsolver and Huey 2008), and the second assumption then predicts that increased temperature leads to faster juvenile

growth and slower adult growth (Morita et al. 2010), which has sometimes been called the "temperature-size rule" (Oke et al. 2022). We therefore recommend future research to incorporate a temperature-dependent link in both anabolism and catabolism parameters ($H$ and $K$ in Equation 1). This would then allow future studies to investigate the impact of ocean temperature on fish productivity via both forage availability (population-level consumption) as well as bioenergetics (individual-level metabolism and foraging rates).

Despite these ecological and management reasons to study bottom-up drivers for weight-at-age, we note several drawbacks in the implementation involving Ecostate. Most significantly, fishery mortality must be assigned a priori to a given stanza, and therefore fishery selectivity cannot be estimated using an age- or length-based function as is common in age-structured models. Future research could relax this assumption; although it would require some restructuring in how age-structured fishing mortality (Equation 6) is represented when integrating biomass dynamics for all functional groups (Equation 2). We also have not represented demographic differences in sexually dimorphic species (e.g., sablefish). Future research could approximate this by representing males and females as separate age-structured populations. However, this would require modifications to allow recruitment deviations to be shared across sexes as well as different processing of data inputs (e.g., developing abundance indices by sex). Additionally, we have not added detailed indexing for multiple survey and fishery fleets to the software package Ecostate; although this does not pose any fundamental difficulties beyond a more complex user interface. Finally, we have not incorporated handling time adjustments, which allow an increase in available prey to cause a decrease in predation mortality instead of an increase in individual growth. EwE includes many options for complicated functional responses (Christensen and Walters 2004), and future research could add and then test these features in a state-space model such as Ecostate.

We encourage further research to fit directly to consumption data resulting from stomach content and diet samples. Stomach-content data can be standardised to estimate annual variation in both consumption and diet. We envision that these data could be fitted either as an index of total consumption and compositional data regarding diet proportions, or alternatively as a set of indices of prey-specific consumption. These two alternative options are somewhat analogous to the split between fitting age-based survey data as an abundance index and age-compositions, or as a matrix of abundance-at-age, and there are benefits and drawbacks to both approaches (Thorson et al. 2023). Regardless of which parameterisation is used, we envision that stomach-content data could be used to identify prey-switching, temperature-dependent changes in consumption, and other realistic complications that arise in trophic ecology. For example, fitting stomach-content data could allow future research to estimate the degree to which increased prey availability translates to greater consumption (i.e., increased individual growth) vs. decreased foraging time (i.e., decreased predation mortality). We hope that (1) greater flexibility in representing predator consumption combined with (2) diet and consumption data from stomach contents will then allow future studies to better match observed variation in predator weight-at-age.

## Conflicts of Interest

The authors declare no conflicts of interest.

## Data Availability Statement

All analysis was conducted using the R-package *ecostate*, release 0.2.0, available on GitHub (https://github.com/James-Thorson-NOAA/ecostate) and CRAN (https://cran.r-project.org/web/packages/ecostate/index.html) and with additional vignettes available via pkgdown (https://james-thorson-noaa.github.io/ecostate/). Code and Gulf of Alaska data to replicate the analysis are available as vignette "age-structured and bottom-up interactions" in *ecostate* release 0.3.0.

## Endnotes

[1] https://james-thorson-noaa.github.io/ecostate/articles/model-description.html.

[2] In the following, we use vector–matrix notation (see Edwards and Auger-Méthé 2019), but introduce binary subscripts $s2$, $g2$, etc., due to running out of Roman letters for data and subscripts.

## References

Adams, G. D., K. K. Holsman, S. J. Barbeaux, et al. 2022. "An Ensemble Approach to Understand Predation Mortality for Groundfish in the Gulf of Alaska." *Fisheries Research* 251: 106303. https://doi.org/10.1016/j.fishres.2022.106303.

Atkinson, R., A. G. Gaedke, U. Sprules, et al. 2024. "Steeper Size Spectra With Decreasing Phytoplankton Biomass Indicate Strong Trophic Amplification and Future Fish Declines." *Nature Communications* 15, no. 1: 381. https://doi.org/10.1038/s41467-023-44406-5.

Begley, J., and D. Howell. 2004. "*An Overview of Gadget, the Globally Applicable Area-Disaggregated General Ecosystem Toolbox.*" https://imr.brage.unit.no/imr-xmlui/bitstream/handle/11250/100625/FF1304.pdf?sequence=1.

Bentley, J. W., D. Chagaris, M. Coll, et al. 2024. "Calibrating Ecosystem Models to Support Ecosystem-Based Management of Marine Systems." *ICES Journal of Marine Science* 81, no. 2: 260–275. https://doi.org/10.1093/icesjms/fsad213.

Bentley, J. W., M. G. Lundy, D. Howell, et al. 2021. "Refining Fisheries Advice With Stock-Specific Ecosystem Information." *Frontiers in Marine Science* 8. https://doi.org/10.3389/fmars.2021.602072.

Bertalanffy, L. V. 1969. *General System Theory: Foundations, Development, Applications*. Revised ed. George Braziller Inc.

Boyce, D. G., and B. Worm. 2015. "Patterns and Ecological Implications of Historical Marine Phytoplankton Change." *Marine Ecology Progress Series* 534: 251–272. https://doi.org/10.3354/meps11411.

Carvalho, F., H. Winker, D. Courtney, et al. 2021. "A Cookbook for Using Model Diagnostics in Integrated Stock Assessments." *Fisheries Research* 240: 105959. https://doi.org/10.1016/j.fishres.2021.105959.

Chagaris, D., K. Drew, A. Schueller, M. Cieri, J. Brito, and A. Buchheister. 2020. "Ecological Reference Points for Atlantic Menhaden Established Using an Ecosystem Model of Intermediate Complexity." *Frontiers in Marine Science* 7: 606417. https://doi.org/10.3389/fmars.2020.606417.

Chassot, E., S. Bonhommeau, N. K. Dulvy, et al. 2010. "Global Marine Primary Production Constrains Fisheries Catches." *Ecology Letters* 13, no. 4: 495–505. https://doi.org/10.1111/j.1461-0248.2010.01443.x.

Cheng, M., D. R. Goethel, P.-J. F. Hulson, K. B. Echave, and C. J. Cunningham. 2024. "'Slim Pickings?': Extreme Large Recruitment Events May Induce Density-Dependent Reductions in Growth for Alaska Sablefish (*Anoplopoma fimbria*) With Implications for Stock Assessment." *Canadian Journal of Fisheries and Aquatic Sciences* 82: 1–13. https://doi.org/10.1139/cjfas-2024-0228.

Christensen, V., and C. J. Walters. 2004. "Ecopath With Ecosim: Methods, Capabilities and Limitations." *Ecological Modelling* 172, no. 2: 109–139. https://doi.org/10.1016/j.ecolmodel.2003.09.003.

Correa, G. M., C. C. Monnahan, J. Y. Sullivan, J. T. Thorson, and A. E. Punt. 2023. "Modelling Time-Varying Growth in State-Space Stock Assessments." *ICES Journal of Marine Science* 80, no. 7: 2036–2049. https://doi.org/10.1093/icesjms/fsad133.

Cushing, D. H. 1990. "Plankton Production and Year-Class Strength in Fish Populations: An Update of the Match/Mismatch Hypothesis." *Advances in Marine Biology* 26: 249–293.

Edwards, A. M., and M. Auger-Méthé. 2019. "Some Guidance on Using Mathematical Notation in Ecology." *Methods in Ecology and Evolution* 10, no. 1: 92–99. https://doi.org/10.1111/2041-210X.13105.

Essington, T. E., J. F. Kitchell, and C. J. Walters. 2001. "The von Bertalanffy Growth Function, Bioenergetics, and the Consumption Rates of Fish." *Canadian Journal of Fisheries and Aquatic Sciences* 58, no. 11: 2129–2138.

Fitzpatrick, K. B., B. C. Weidel, M. J. Connerton, et al. 2022. "Balancing Prey Availability and Predator Consumption: A Multispecies Stock Assessment for Lake Ontario." *Canadian Journal of Fisheries and Aquatic Sciences* 79, no. 9: 1529–1545. https://doi.org/10.1139/cjfas-2021-0126.

Goethel, D. R., D. H. Hanselman, C. J. Rodgveller, et al. 2024. "*Assessment of the Sablefish Stock in Alaska.*" https://www.researchgate.net/profile/Matthew-Cheng-15/publication/370978839_2022_Alaska_Sablefish_Stock_Assessment_and_Fishery_Evaluation_SAFE_Report/links/646d2cb937d6625c002c5dae/2022-Alaska-Sablefish-Stock-Assessment-and-Fishery-Evaluation-SAFE-Report.pdf.

Hipsey, M. R., G. Gal, G. B. Arhonditsis, et al. 2020. "A System of Metrics for the Assessment and Improvement of Aquatic Ecosystem Models." *Environmental Modelling & Software* 128: 104697. https://doi.org/10.1016/j.envsoft.2020.104697.

Hopcroft, R. R. 2023. "Spring and Fall Large Copepod and Euphausiid Biomass: Seward Line." In *Ecosystem Status Report 2023: Gulf of Alaska, Stock Assessment and Fishery Evaluation Report*, edited by B. Ferriss. North Pacific Fishery Management Council.

Jurado-Molina, J., P. A. Livingston, and J. N. Ianelli. 2005. "Incorporating Predation Interactions in a Statistical Catch-At-Age Model for a Predator-Prey System in the Eastern Bering Sea." *Canadian Journal of Fisheries and Aquatic Sciences* 62, no. 8: 1865–1873.

Kapur, M. S., N. Ducharme-Barth, M. Oshima, and F. Carvalho. 2025. "Good Practices, Trade-Offs, and Precautions for Model Diagnostics in Integrated Stock Assessments." *Fisheries Research* 281: 107206. https://doi.org/10.1016/j.fishres.2024.107206.

Karp, M. A., J. S. Link, M. Grezlik, et al. 2023. "Increasing the Uptake of Multispecies Models in Fisheries Management." *ICES Journal of Marine Science* 80, no. 2: 243–257. https://doi.org/10.1093/icesjms/fsad001.

Kimmel, D., K. Axler, B. Cormack, et al. 2023. "Current and Historical Trends for Zooplankton in the Western Gulf of Alaska." In

*Ecosystem Status Report 2023: Gulf of Alaska, Stock Assessment and Fishery Evaluation Report*, edited by B. Ferris. North Pacific Fishery Management Council.

Kingsolver, J., and R. Huey. 2008. "Size, Temperature, and Fitness: Three Rules." *Evolutionary Ecology Research* 10, no. 2: 251–268.

Kristensen, K. 2014. "TMB: General Random Effect Model Builder Tool Inspired by ADMB." https://github.com/kaskr/adcomp.

Kristensen, K. 2024. "RTMB: "R" Bindings for "TMB"." https://CRAN.R-project.org/package=RTMB.

Leroux, S. J., and M. Loreau. 2015. "Theoretical perspectives on bottom-up and top-down interactions across ecosystems." In *Trophic ecology: Bottom-up and Top-down Interactions across Aquatic and Terrestrial Systems*, edited by T. C. Hanley and K. J. La Pierre, 3–28. Cambridge University Press.

Lucey, S. M., S. K. Gaichas, and K. Y. Aydin. 2020. "Conducting Reproducible Ecosystem Modeling Using the Open Source Mass Balance Model Rpath." *Ecological Modelling* 427: 109057. https://doi.org/10.1016/j.ecolmodel.2020.109057.

Melnychuk, M. C., H. Kurota, P. M. Mace, et al. 2021. "Identifying Management Actions That Promote Sustainable Fisheries." *Nature Sustainability* 4, no. 5: 440–449. https://doi.org/10.1038/s41893-020-00668-1.

Methot, R. D. 2009. "Stock Assessment: Operational Models in Support of Fisheries Management." In *The Future of Fisheries Science in North America*, edited by R. J. Beamish and B. J. Rothschild, vol. 31, 137–165. Springer Netherlands.

Methot, R. D., and I. G. Taylor. 2011. "Adjusting for Bias due to Variability of Estimated Recruitments in Fishery Assessment Models." *Canadian Journal of Fisheries and Aquatic Sciences* 68, no. 10: 1744–1760.

Monnahan, C. C., G. D. Adams, B. E. Ferriss, S. K. Shotwell, D. R. McKelvey, and D. W. McGowan. 2023. "*Assessment of the Walleye Pollock Stock in the Gulf of Alaska* (Stock Assessment and Fishery Evaluation Report for Groundfish Resources of the Gulf of Alaska)." North Pacific Fishery Management Council. https://apps-afsc.fisheries.noaa.gov/Plan_Team/2021/GOApollock.pdf.

Monnahan, C. C., and K. Kristensen. 2018. "No-U-Turn Sampling for Fast Bayesian Inference in ADMB and TMB: Introducing the Adnuts and Tmbstan R Packages." *PLoS One* 13, no. 5: e0197954. https://doi.org/10.1371/journal.pone.0197954.

Morita, K., M. Fukuwaka, N. Tanimata, and O. Yamamura. 2010. "Size-Dependent Thermal Preferences in a Pelagic Fish." *Oikos* 119, no. 8: 1265–1272. https://doi.org/10.1111/j.1600-0706.2009.18125.x.

Neuenfeldt, S., V. Bartolino, A. Orio, et al. 2020. "Feeding and Growth of Atlantic Cod (*Gadus morhua* L.) in the Eastern Baltic Sea Under Environmental Change." *ICES Journal of Marine Science* 77, no. 2: 624–632. https://doi.org/10.1093/icesjms/fsz224.

Oke, K. B., F. Mueter, and M. A. Litzow. 2022. "Warming Leads to Opposite Patterns in Weight-At-Age for Young Versus Old Age Classes of Bering Sea Walleye Pollock." *Canadian Journal of Fisheries and Aquatic Sciences* 79, no. 10: 1655–1666. https://doi.org/10.1139/cjfas-2021-0315.

Polovina, J. J. 1984. "Model of a Coral Reef Ecosystem." *Coral Reefs* 3, no. 1: 1–11. https://doi.org/10.1007/BF00306135.

Punt, A. E., A. Dunn, B. Þ. Elvarsson, et al. 2020. "Essential Features of the Next-Generation Integrated Fisheries Stock Assessment Package: A Perspective." *Fisheries Research* 229: 105617. https://doi.org/10.1016/j.fishres.2020.105617.

Scott, E., N. Serpetti, J. Steenbeek, and J. J. Heymans. 2016. "A Stepwise Fitting Procedure for Automated Fitting of Ecopath With Ecosim Models." *SoftwareX* 5: 25–30. https://doi.org/10.1016/j.softx.2016.02.002.

Siple, M. C., P. G. von Szalay, N. W. Raring, A. N. Dowlin, and B. C. Riggle. 2024. "*Data Report: 2023 Gulf of Alaska Bottom Trawl Survey* (Nos. 2024-09; AFSC Processed Rep., p. 145)." Alaska Fisheries Science Center, National Marine Fisheries Service. https://repository.library.noaa.gov/view/noaa/61491.

Stock, B. C., H. Xu, T. J. Miller, J. T. Thorson, and J. A. Nye. 2021. "Implementing Two-Dimensional Autocorrelation in Either Survival or Natural Mortality Improves a State-Space Assessment Model for Southern New England-Mid Atlantic Yellowtail Flounder." *Fisheries Research* 237: 105873. https://doi.org/10.1016/j.fishres.2021.105873.

Thorson, J. T., K. F. Johnson, R. D. Methot, and I. G. Taylor. 2017. "Model-Based Estimates of Effective Sample Size in Stock Assessment Models Using the Dirichlet-Multinomial Distribution." *Fisheries Research* 192: 84–93. https://doi.org/10.1016/j.fishres.2016.06.005.

Thorson, J. T., K. Kristensen, K. Y. Aydin, et al. 2024. "The Benefits of Hierarchical Ecosystem Models: Demonstration Using EcoState, a New State-Space Mass-Balance Model." *Fish and Fisheries* 26: 203–218. https://doi.org/10.1111/faf.12874.

Thorson, J. T., C. C. Monnahan, and P.-J. F. Hulson. 2023. "Data Weighting: An Iterative Process Linking Surveys, Data Synthesis, and Population Models to Evaluate Mis-Specification." *Fisheries Research* 266: 106762. https://doi.org/10.1016/j.fishres.2023.106762.

Trathan, P. N., V. Warwick-Evans, E. F. Young, A. Friedlaender, J. H. Kim, and N. Kokubun. 2022. "The Ecosystem Approach to Management of the Antarctic Krill Fishery—The 'Devils Are in the Detail' at Small Spatial and Temporal Scales." *Journal of Marine Systems* 225: 103598. https://doi.org/10.1016/j.jmarsys.2021.103598.

Tulloch, V. J. D., É. E. Plagányi, C. Brown, A. J. Richardson, and R. Matear. 2019. "Future Recovery of Baleen Whales Is Imperiled by Climate Change." *Global Change Biology* 25, no. 4: 1263–1281. https://doi.org/10.1111/gcb.14573.

Von Bertalanffy, L. 1960. "Fundamental Aspects of Normal and Malignant Growth." *Principles and Theory of Growth* 493: 137–259.

Walters, C., V. Christensen, and D. Pauly. 1997. "Structuring Dynamic Models of Exploited Ecosystems From Trophic Mass-Balance Assessments." *Reviews in Fish Biology and Fisheries* 7, no. 2: 139–172. https://doi.org/10.1023/A:1018479526149.

Walters, C., and J. F. Kitchell. 2001. "Cultivation/Depensation Effects on Juvenile Survival and Recruitment: Implications for the Theory of Fishing." *Canadian Journal of Fisheries and Aquatic Sciences* 58, no. 1: 39–50.

Walters, C., D. Pauly, V. Christensen, and J. F. Kitchell. 2000. "Representing Density Dependent Consequences of Life History Strategies in Aquatic Ecosystems: EcoSim II." *Ecosystems* 3, no. 1: 70–83. https://doi.org/10.1007/s100210000011.

## Supporting Information

Additional supporting information can be found online in the Supporting Information section. **Appendix S1:** faf70016-sup-0001-supinfo.docx.